Restoration of Drift Signal using VAE-LSTM

Eunse Ahn [a], Hee-Jae Lee [a], Hyojin Kim[a], Jonghyun Kim [a*]
[a]Chosun University, 309 Pilmun-daero, Dong-gu, Gwangju, 61452, Republic of Korea
*[*]Corresponding author: jonghyun.kim@chosun.ac.kr**

1. Introduction

Nuclear power plants (NPP) are complex systems equipped with numerous sensors that play a vital role in their operation. Since operators rely on the information provided by these signals to operate NPP, sensor faults can result in providing incorrect information to the operators and thereby leading to improper actions that can affect NPP safety [1]. This can be found in an example in Three Mile Island (TMI) NPP accidents, where incorrect signals to operators were a major contributing factor to catastrophic incidents [2].

Over time, sensors in various instruments may degrade and be affected by vibrations, shocks, and environmental changes, leading to measurement errors [3]. Signal drift, a gradual shift from the expected value, is notably observed in NPPs [4, 5]. To ensure NPP safety, it's crucial to recover these drift signals after detecting them, necessitating the development of a corrective technique.

To address this, several previous studies have proposed signal reconstruction and restoration algorithms using Long Short-Term Memory (LSTM) [6], Generative Adversarial Networks (GAN) [7], 1D Convolutional Neural Networks (1D-CNN) [8], Variable AutoEncoder (VAE) [9] and multivariate autoregressive (MVAR) [10].

Extending these works, this study aims to develop a signal restoration algorithm combining a VAE with an LSTM method. The purpose of the proposed algorithm is to restore drift failures into normal signals during the normal operation. To do this, the authors collected data using an iPWR simulator, which is a kind of small modular reactor (SMR), and then tested it with drift-injected data.

2. Methodology

2.1 LSTM

LSTM, an advanced Recurrent Neural Network (RNN), offers improved long-term data dependencies. Its distinctive feature from RNN is its cell state, which retains information over long sequences [11]. LSTM uses three gates: forget, input, and output. The forget gate decides what to discard from the cell state using a sigmoid function. The input gate uses both sigmoid and tanh functions to update the cell state. The output gate sets the next hidden state's value based on current cell state. The structure of an LSTM is shown in Fig. 1.
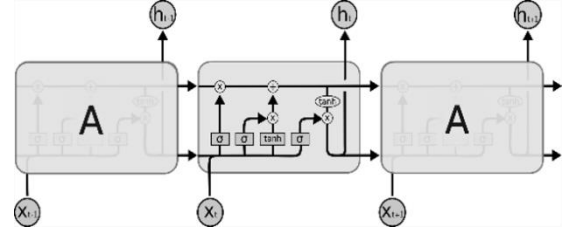

Fig. 1. LSTM Architecture.

2.2 VAE

VAE is one of variational inference techniques that have been used for image and signal restoration [12]. VAE employs an encoder and decoder, which allows it to compress features from input into a latent space and subsequently generate data to be similar to the input. An encoder in VAE extracts a normal distribution using mean μ and variance σ with the encoder function, $q_\phi(z|x)$. Then the decoder approximates the posterior distribution with $p_\theta(z|x)$. VAE samples a latent vector (appear in z in Fig. 2.) which follows the normal distribution. As a result, a decoder produce a reconstructed output x'.
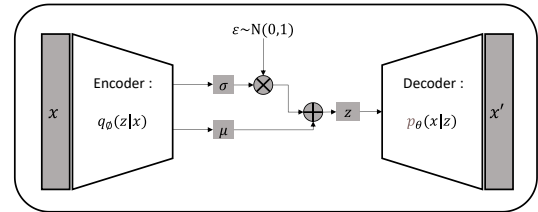

Fig. 2. VAE Architecture.

3. Signal Restoration Algorithm for Drift Signal

The objective of this algorithm is to restore a drift signal to its correct signal when drift occurs during normal operation. As illustrated in Fig. 3, the algorithm consists of three steps: 1) pre-processing, 2) restoration of faulty signal, and 3) validation of restored faulty signal.
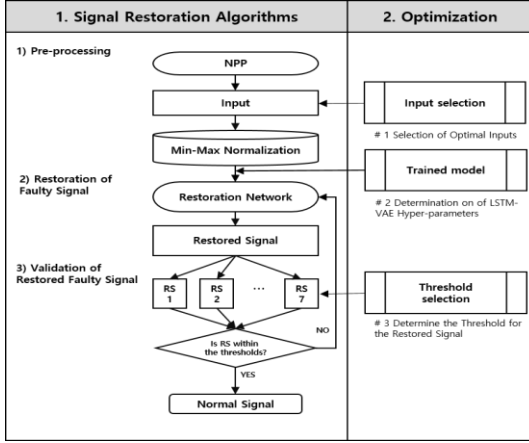
Fig. 3. The proposed signal restoration algorithm for drift signals in normal operation.

3.1 Pre-processing

Pre-processing involves input selection, noise injection, drift injection, and data normalization. Key input variables were selected through a procedure analysis based on the Integral Pressurized Water Reactor (iPWR) Simulator Handbook [13] and system analysis using the iPWR simulator, resulting in 100 chosen variables.

Since signals in actual NPPs include noises due to various factors [14], this study artificially introduced White Gaussian noise into simulator data, assuming a standard deviation of 0.001 for input values.

Min-max normalization adjusts data to a 0-1 scale to mitigate varied input scales' impact on AI training, as described in Eq. 1. In Eq.1. X is the original value, X_{min} is the minimum value in the dataset, X_{max} is the maximum value in the dataset and X_{Norm} is the normalized value.

$$(1)\ X_{Norm} = \frac{(X - X_{min})}{(X_{max} - X_{min})}$$

3.2 Restoration Network

The network proposed in this study utilizes VAE combining with LSTM as illustrated in Fig. 4. The objective of this network to generate restored data resembling normal signals from the drift signal.
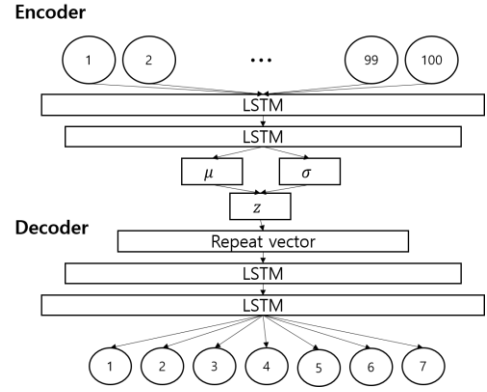

Fig 4. VAE-LSTM Network Structure.

3.3 Validation of restored faulty signal

The validation of restored data checks if within a set boundary. If within the threshold, it's used as a normal signal; if not, the proposed network performs signal restoration.

4. Training and Experiment
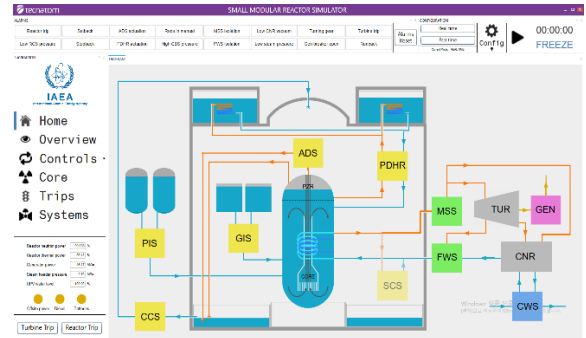
4.1 Training and Optimization

Fig 5. iPWR Simulator.

The training and testing data were collected using the iPWR simulator that is a kind of SMR developed by Tecnatom. Fig. 5 shows the main display of the iPWR simulator. A total of 50 datasets were collected for a normal scenario, beginning-of-life 100% with forced circulation operation. Each dataset includes 10-minute normal operation. Among the datasets, 40 datasets (80%) and 10 datasets (20%) were used for training and validation, respectively.

To improve the performance of the proposed network, this study performed optimizations for model hyperparameters (e.g. sequence, batch, layer, and L_{VAE}). The performances were measured by combining reconstruction and KL divergence errors. Reconstruction error measures input-output discrepancies, while KL divergence contrasts latent variable distributions. The combined loss can be calculated as Eq. 2-5. In Eq. 2~3 x_i represents the ith element of the original data, while x_i' denotes the ith element of the reconstructed data. In

Eq. 4, μ_j and σ_j represent the mean and variance of the jth dimension of the latent variable, respectively.

(2) $L_{rec} = -\Sigma_i(x_i log(x_i') + (1 - x_i)log(1 - x_i'))$
(3) $L_{rec} = \Sigma_i(x_i - x_i')$
(4) $L_{KL} = \frac{1}{2}\Sigma_j(1 + log(\sigma_j^2) - \mu_j^2 - \sigma_j^2)$
(5) $L_{VAE} = L_{rec} + L_{KL}$

Table 1: Model Optimization

No.	Sequence	Batch	Layer	L_{VAE}
1	5	32	7	6.1493e-05
2	10	32	7	1.7460e-04
3	10	32	9	1.9730e-04
4	5	64	9	8.0142e-05
5	10	64	7	1.1493e-05
6	10	64	9	6.1839e-05
7	5	256	9	1.8210e-06
8	10	256	9	1.3362e-06
9	15	512	10	4.6030e-05
10	15	256	9	4.8383e-05

4.2 Fault Signal Injection

The drift signal was injected into the normal data by multiplying it with a pre-set drift ratio at each time point. The injection of the drift signal started 60 seconds after the beginning of the scenario and was set to increase by 0.001% per second.

4.3 Threshold

The threshold plays a role in determining whether the restored data is reliable. This study sets the threshold as the sensor's allowable error range, 0.25% for normal signals.

4.4 Result

The trained algorithm was tested with a drift signal artificially injected, and its restoration accuracy was assessed using the Mean Square Error (MSE). Table 2 and Fig. 6 shows the calculated MSE and the restored results.
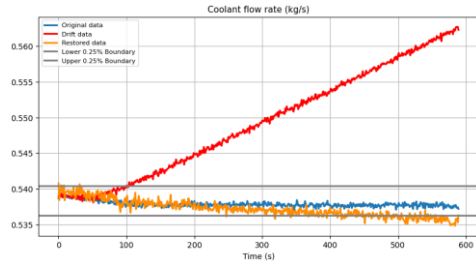
Table 2: MSE values for variables

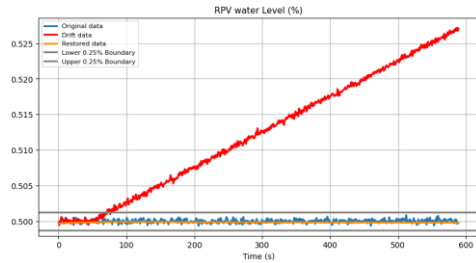| No.	Variable	MSE
1	Steam pressure line 1 (MPa)	0.0002
2	Steam pressure line 2 (MPa)	0.0002
3	Coolant flow rate (kg/s)	0.0014
4	RPV Water Level (%)	2.51E-05
5	PZR Level (%)	4.71E-05
6	RPV Pressure (MPa)	2.49E-05
7	Coolant Temperature at core outlet (ºc)	4.16E-05
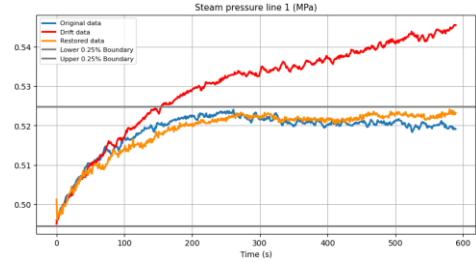
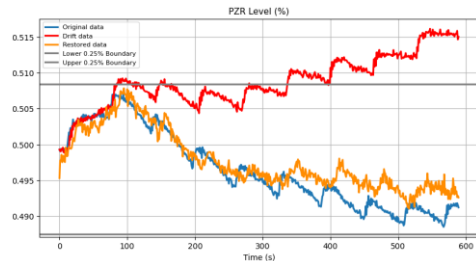(a)   Steam pressure line 1 (MPa).
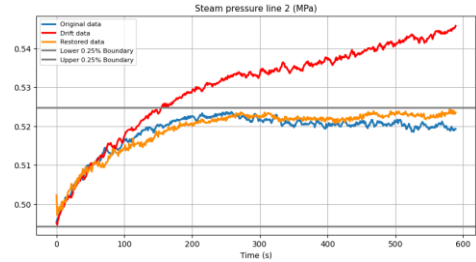
(b)   Steam pressure line 2 (MPa).
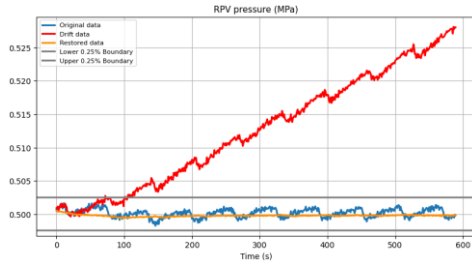

(c)   Coolant flow rate (kg/s).
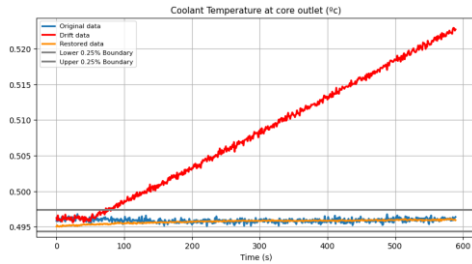

(d)   RPV water Level (%).

(e)   PZR Level (%).

(f)   RPV pressure (MPa).

(g)   Coolant Temperature at core outlet (ºc).

Fig 6. Comparisons of the restored data (orange), the drift-injected data (red) with original data (blue).

4. Conclusions

In this paper, an algorithm is proposed to restore Drift faults from normal signals to their original state using the VAE-LSTM model. The test result indicated that the proposed algorithm successfully restored all seven output variables within the designated threshold. Additionally, leveraging the inherent characteristics of the VAE model, noise was eliminated to yield more accurate information in the results. Through validation, it was demonstrated that the proposed algorithm achieves its intended high-quality restoration performance. Therefore, this algorithm can provide operators with more accurate information during normal nuclear power plant operations when a drift fault occurs.

5. Acknowledgments

REFERENCES

[1] J. Choi, & S. J. Lee, Consistency index-based sensor fault detection system for nuclear power plant emergency situations using an LSTM network, Sensors, 20(6), 1651, 2020.
[2] B. A. Osif, A. J. Baratta, & T. W. Conkling, TMI 25 years later: The Three Mile Island nuclear power plant accident and its impact, Penn State Press, 2004.
[3] N. S. Rao, C. Greulich, P. Ramuhalli, S. M. Cetiner, & P. Devineni, Sensor drift estimation for reactor systems by fusing multiple sensor measurements, In 2019 IEEE Nuclear Science Symposium and Medical Imaging Conference (NSS/MIC) (pp. 1-2), IEEE, 2019.
[4] D. Kumar, S. Rajasegarar, & M. Palaniswami, Automatic sensor drift detection and correction using spatial kriging and kalman filtering, In 2013 IEEE International Conference on Distributed Computing in Sensor Systems (pp. 183-190), IEEE, 2013.
[5] Y. Choi, G. Yoon, & J. Kim, Unsupervised learning algorithm for signal validation in emergency situations at nuclear power plants, Nuclear Engineering and Technology, 54(4), 1230-1244, 2022.
[6] Y. N. Zhou, S. Wang, T. Wu, L. Feng, W. Wu, J. Luo,,... & N. N. Yan, For-backward LSTM-based missing data reconstruction for time-series Landsat images, GIScience & Remote Sensing, 59(1), 410-430, 2022.
[7] S. G. Kim, Y. H. Chae, & P. H. Seong, Development of a generative-adversarial-network-based signal reconstruction method for nuclear power plants, Annals of Nuclear Energy, 142, 107410, 2020.
[8] Z. Yang, P. Xu, B. Zhang, C. Xu, L. Zhang, H. Xie, & Q. Duan, Nuclear power plant sensor signal reconstruction based on deep learning methods, Annals of Nuclear Energy, 167, 108765, 2022.
[9] L. Jiang, B. Dai, W. Wu, & C. C. Loy, Focal frequency loss for image reconstruction and synthesis, In Proceedings of the IEEE/CVF International Conference on Computer Vision (pp. 13919-13929), 2021.
[10] T. H. Lin, & S. C. Wu, Sensor fault detection, isolation and reconstruction in nuclear power plants, Annals of Nuclear Energy, 126, 398-409, 2019.
[11] T. Fischer, & C. Krauss, Deep learning with long short-term memory networks for financial market predictions, European journal of operational research, 270(2), 654-669, 2018.
[12] Diederik P. Kingma, and Max Welling, Auto-encoding variational bayes, arXiv preprint arXiv:1312.6114, 2013.
[13] INTERNATIONAL ATOMIC ENERGY AGENCY, Integral Pressurized Water Reactor Simulator Manual: Exercise Handbook, Training Course Series No. 65, IAEA, Vienna, 2017.
[14] B. Yang, H. Xia, M. Annor-Nyarko, & Z. Wang, Application of total variation denoising in nuclear power plant signal pre-processing, Annals of Nuclear Energy, 135, 106981, 2020.